



Molecular dynamics study on Revaprazan and its analogue as potassium-competitive acid blockers

Fei Ren¹, Zi-Qiang Wu¹, Hua-Jun Luo^{1*} and Wei-Qiao Deng^{1,2}

¹College of Biological and Pharmaceutical Science, China Three Gorges University, Yichang, China

²State Key Laboratory of Molecular Reaction Dynamics, Dalian Institute of Chemical Physics, Chinese Academy of Sciences, Dalian, China

ABSTRACT

The interaction mechanisms of revaprazan and its analogue revaprazan-7h as potassium-competitive acid blockers (P-CABs) were studied by induced-fit docking, molecular dynamics and MM/GBSA binding free energy calculation methods. The order of favorable binding interaction is revaprazan-7h (neutral form) > revaprazan (protonated form) > revaprazan-7h (protonated form) > revaprazan (neutral form). The calculation results indicate that enlarging the binding region of ligand with H⁺,K⁺-ATPase (such as residues Thr134, Thr135, Asp137, Asn138, Trp899, Glu900, Gln924, Tyr928, Phe988 and Asn989) would increase the activity. Due to hydrogen bonds and electrostatic interactions, Asp137 in particular should be a very important binding site for protonated form of ligand. The findings could help for further rational design of novel P-CABs.

Keywords: Revaprazan; Potassium-competitive acid blockers; Molecular dynamics; protonated form; H⁺,K⁺-ATPase

INTRODUCTION

The gastric H⁺,K⁺-ATPase (proton pump) is the key therapeutic target for the ulcer diseases such as gastric ulcers, duodenal ulcers, gastro esophageal reflux disease (GERD), and so on [1-3]. It is a dimeric heterodimer composed of α subunit of about 1033 amino acids with 10 transmembrane (TM) segments and β -subunit glycoprotein with 290 amino acids [4,5], which engages in 2K⁺/2H⁺/1ATP electroneutral ion exchange to generate a million-fold H⁺-gradient across the mammalian canalicular membrane of the parietal cell [6,7].

Proton pump inhibitors (PPIs) such as omeprazole, lansoprazole, rabeprazole, pantoprazole, tenatoprazole and leminoprazole are considered as the first-line therapy for acid suppression [8]. However, PPIs exhibit a delayed onset of acute effect and achieve full effect only slowly and incrementally over several dose cycles [9], primarily due to their chemical structures and irreversible inhibition of H⁺,K⁺-ATPase [10,11]. Now potassium-competitive acid blockers (P-CABs) are found to overcome the limitations of PPIs, which reversibly inhibit gastric H⁺,K⁺-ATPase by competing with the K⁺ on the luminal surface and provide faster onset and longer duration of action than conventional PPIs [9]. Revaprazan (IC₅₀ = 0.350 μ M at pH 6.1) (Fig. 1) is the first P-CAB used clinically in 2007 for the treatment of duodenal ulcer, gastric ulcer and gastritis, and is undergoing phase III clinical studies for the treatment of GERD [12, 13]. Yoon *et al.* [14] then synthesized revaprazan-7h (Fig. 1) as revaprazan analogue in 2010, which has higher activity (IC₅₀ = 0.052 μ M at pH 6.1). Although these compounds are all weak bases and have a little difference in chemical structure, they are significantly different in the inhibition activity. According to the pKa calculation using ACD/I-Lab [15], revaprazan and revaprazan-7h have pKa values of 7.26 \pm 0.10 and 5.60 \pm 0.40, which are 69.89% and 26.04% protonated at pH 6.1, respectively. Hence there are two forms (neutral and protonated forms) of the compounds interacting with H⁺,K⁺-ATPase.

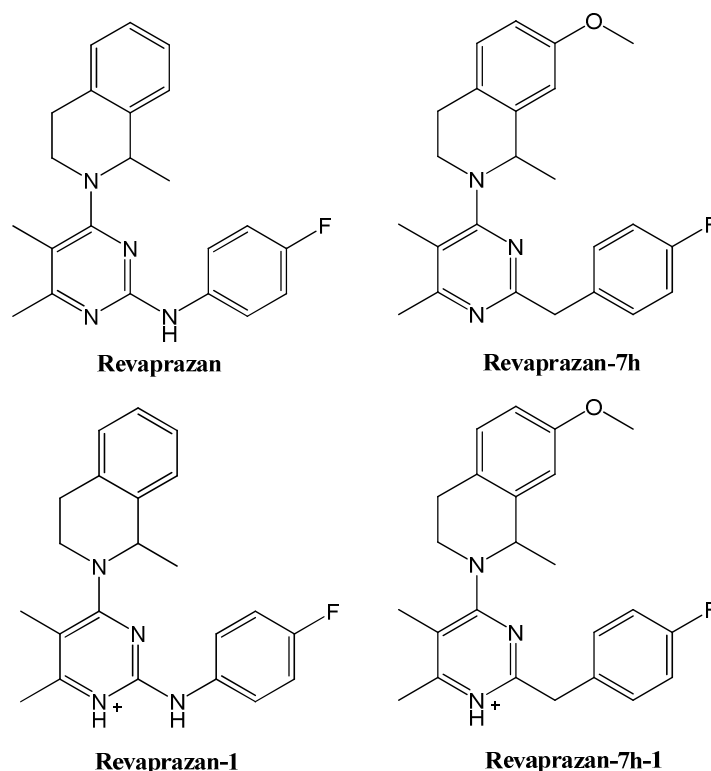


Fig.1. Chemical structures of revaprazan and revaprazan-7h with their protonated form

So far the structure of gastric H^+,K^+ -ATPase is poorly defined, being currently limited to a resolution of 7 Å (PDB code: 3IXZ [16], resolution: 6.5 Å; PDB code: 2XZB [17], resolution: 7 Å). So the aim of this paper is to model H^+,K^+ -ATPase structure by homology modeling and to investigate the different interactions between H^+,K^+ -ATPase and revaprazan (revaprazan-7h) including neutral and protonated forms using molecular docking, molecular dynamics and MM/GBSA calculation methods.

EXPERIMENTAL SECTION

Homology modeling

The sequence of the pig gastric H^+,K^+ -ATPase (1033 amino acids) was taken from the Swiss-Prot Database (ID: P09626) [18]. From the Protein Data Bank [19], the crystal structure of Na^+,K^+ -ATPase in the E_2P state (PDB code: 2ZXE) [20] was used as a template by BLAST online method (<http://blast.ncbi.nlm.nih.gov/Blast.cgi>) [21]. The sequence alignment was performed with the ClustalW2 algorithm [22]. The homology model of pig H^+,K^+ -ATPase was generated using MODELLER9v4 [23]. The resultant structure of the H^+,K^+ -ATPase was subject to the Protein Preparation Wizard module in Schrödinger [24] as follows: adding hydrogens, assigning partial charges, and minimizing using the OPLS-2005 force field [25] until RMSD 0.30 Å. The final optimized model was validated using the program PROCHECK [26] to assess the quality of the stereochemistry of the protein structure.

Ligands preparation

LigPrep of Schrödinger software suit [27] was used for the preparation of revaprazan and revaprazan-7h: generating 3D structures from 2D (SDF) representation, and performing energy minimization using MacroModel module of Schrödinger. Truncated Newton Conjugate Gradient (TNCG) minimization method was used with 500 iterations and convergence threshold of 0.05 (kJ/mol). While Epik [28] was used to generate possible ionization states at $pH\ 7.0 \pm 1.0$.

Molecular docking

The docking simulations were performed using induced-fit docking (IFD) method [29] in the Schrödinger software suite [24], which had been reported to be a robust and accurate method to account for both ligand and receptor flexibility [29,30]. The IFD protocol was carried out in three consecutive steps [31,32]. Firstly, the ligand was docked into a rigid receptor model with scaled-down van der Waals (vdW) radii. A vdW scaling of 0.5 was used for both the protein and ligand non-polar atoms. The Glide XP mode [33,34] was used for the initial docking, and 20 ligand poses were retained for protein structural refinements. Previous biochemical and mutagenesis studies [17,35-39] suggest that Ala335, Tyr799 and Cys813 in pig H^+,K^+ -ATPase are the key amino acid residues in the

luminal cavity. Therefore, dimensions for the cubic boundary box centered on the centroid of these three residues were set to 22 Å × 22 Å × 22 Å. Secondly, Prime program was used to generate the induced-fit protein–ligand complexes. Each of the 20 structures from the previous step was subjected to side chain and backbone refinements. All residues with at least one atom located within 5.0 Å of each corresponding ligand pose were included in the Prime refinement [40]. The refined complexes were ranked by Prime energy, and the receptor structures within 30 kcal/mol of the minimum energy structure were passed through for a final round of Glide docking and scoring. Finally, each ligand was redocked into every refined low-energy receptor structure produced in the second step using Glide XP mode at default settings. An IFD score (IFD score = 1.0 Glide_Gscore + 0.05 Prime_Energy) that accounts for both the protein–ligand interaction energy and the total energy of the system was calculated and used to rank the IFD poses. The best pose complex was chosen to run molecular dynamics.

Molecular dynamics

The docking models were subjected to molecular dynamics simulations using Desmond [41,42]. The system was embedded in the POPC (1-palmitoyl-2-oleoyl-*sn*-glycero-3-phosphatidylcholine) bilayer membrane and solvated with an orthorhombic box of SPC water molecules (buffer distance: 8 Å × 8 Å × 10 Å). Counter-ions (Na⁺) were added to neutralize the system and 0.01M KCl was introduced. The final system was composed of approximately 120,000 atoms. Before the simulation, the models were relaxed as follows: (1) two minimization steps (restraining the solute and unrestrained minimization) with maximum runs of 2000 and the convergence threshold for minimization set to 1 kcal/mol/Å. The minimization method was a hybrid of the steepest decent and limited-memory Broyden-Fletcher-Goldfarb-Shanno (LBFSGS) algorithms; (2) after minimization, the simulation in the NVT ensemble was run restraining all solute heavy atoms with temperature of 10 K for 20 ps, using Berendsen thermostat; (3) a simulation in the NPT ensemble restraining all solute heavy atoms with temperature of 10 K and 300K for 20 ps, respectively; (4) a simulation in the NPT ensemble, no restraints, with temperature of 300 K and simulation time of 50 ps. Each model was equilibrated in MD for 20 ns. Then 22 ns MD production runs (time step: 2.0 fs) were performed through NPT ensemble at 300 K with 1.0132 bar pressure. Smooth particle mesh Ewald method (Ewald tolerance: 1e-09) was employed to treat the long-range electrostatic interactions and a 9 Å radius cut off was used for coulombic short range interactions. The energies and frames of each trajectory were recorded every 1 ps and 5 ps, respectively. MD trajectory analysis was performed using Desmond utilities and VMD [43]. The ligand-protein complexes were visualized using PyMOL [44] and analyzed with Ligand Interactions module embedded in Maestro 9.3 [45].

MM/GBSA calculations

Binding free energy (ΔG_{bind}) calculations were performed for 40 snapshots extracted from the last 2 ns stable MD trajectory using molecular mechanics-generalized Born surface area (MM/GBSA) method. MM/GBSA procedure in Prime program [40, 46] was used to calculate ΔG_{bind} of the docked ligands according to the following equations [47]:

$$\Delta G'_{\text{bind}} = \Delta E_{\text{MM}} + \Delta G_{\text{solv}} \quad (1)$$

$$\Delta G_{\text{bind}} = \Delta E_{\text{MM}} + \Delta G_{\text{solv}} - T\Delta S \quad (2)$$

Where ΔE_{MM} is the difference of the gas phase MM energy between the complex and the sum of the energies of the protein and inhibitor, and includes $\Delta E_{\text{internal}}$ (bond, angle, and dihedral energies), ΔE_{Elect} (electrostatic), and ΔE_{VDW} (van der Waals) energies. ΔG_{solv} is the change of the solvation free energy upon binding, and includes the electrostatic solvation free energy ΔG_{GB} (polar contribution calculated using generalized Born model), and the nonelectrostatic solvation component ΔG_{SA} (nonpolar contribution estimated by solvent accessible surface area). $T\Delta S$ is the change of the conformational entropy upon binding, which calculated using normal-mode analysis Rigid Rotor Harmonic Oscillator (RRHO) contained in MacroModel module [48]. $\Delta G'_{\text{bind}}$ neglects the effect of entropy contributions, while ΔG_{bind} includes contributions from loss of ligand translational, rotational and vibrational entropy ($T\Delta S$).

RESULTS AND DISCUSSION

H⁺,K⁺-ATPase homology model

The three-dimensional structure of Na⁺,K⁺-ATPase (PDB code: 2ZXE; resolution: 2.4 Å) [20] was selected as a template, which shares 64% identity to pig H⁺,K⁺-ATPase on the basis of sequence alignment analysis (Fig. 2). The pig gastric H⁺,K⁺-ATPase model is shown in Fig. 3. The stereochemistry of the homology model was assessed using Ramachandran plot generated with the program PROCHECK. The Ramachandran plot indicates that 95.6% of the residues were located in the most favored zones, 4.2% in allowed regions, 0.1% in generously allowed regions and 0.1% in disallowed regions (Fig. 4). The dihedrals, covalent and overall G-factors of this model are 0.16, -0.05 and 0.08, respectively. The PROCHECK G-factors are above -0.5 ideally for the homology model and may therefore be

regarded as structurally realistic.

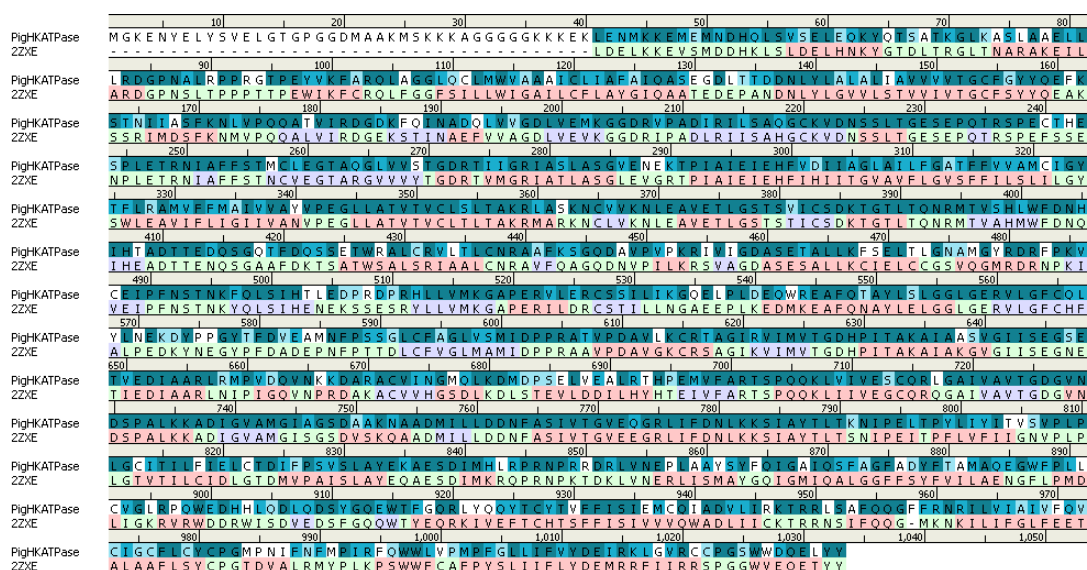


Fig.2. Sequence alignment results between pig H^+,K^+ -ATPase and the template Na^+,K^+ -ATPase (2ZXE). The residues with identical, strong and weak similarities in H^+,K^+ -ATPase are shown in dark blue, blue and light blue color background, respectively. The alpha helical, sheet and coil of secondary structure in the template are colored by pink, light purple and light green

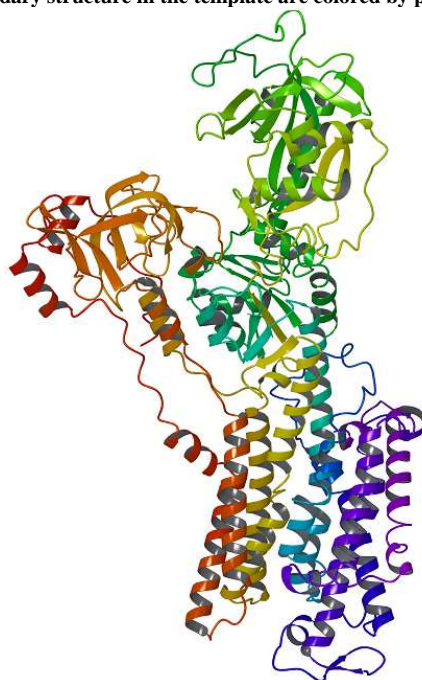


Fig.3. The pig gastric H^+,K^+ -ATPase model

Table 1 Glide docking G Scores and IFD scores of compounds

| Compounds | Gscore | IFD Score |
|-----------------|--------|-----------|
| Revaprazan | -9.41 | -1732.78 |
| Revaprazan-7h | -9.79 | -1732.43 |
| Revaprazan-1 | -8.81 | -1731.30 |
| Revaprazan-7h-1 | -9.36 | -1732.89 |

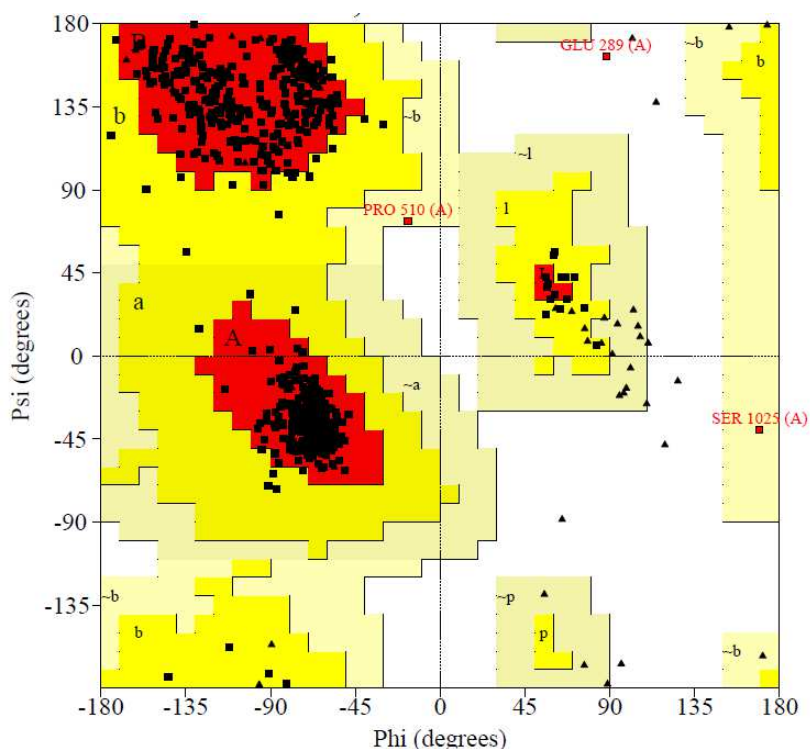


Fig.4. Ramachandran plot of the pig H⁺,K⁺-ATPase model

Molecular docking and molecular dynamics

The molecular docking between H⁺,K⁺-ATPase and compounds was simulated by IFD method. The Glide Gscores and IFD scores (the best pose) of compounds were shown in Table 1. The scores are not significantly different among the compounds. After induced-fit docking, molecular dynamics simulations for the complexes with POPC membrane in 0.01M KCl aqueous solution were run during 22 ns. To check the convergence of calculations and to explore the dynamic stability of complexes, root-mean-square deviations (RMSD) for the backbone atoms from the starting structure were analyzed, as shown in Fig. 5. After 18 ns, The RMSD values for revaprazan, revaprazan-7h, revaprazan-1 and revaprazan-7h-1 system remain 2.92 ± 0.23 Å, 1.91 ± 0.13 Å, 3.10 ± 0.18 Å and 3.27 ± 0.17 Å, respectively. The systems tend to stable and equilibrated. Furthermore, root-mean-square fluctuations (RMSF) versus H⁺,K⁺-ATPase residue number for the complexes are illustrated in Fig. 6. RMSF distributions of the complexes are relatively rigid in the active site region (residues Leu141 in TM2, Ala335 in TM4, Tyr799 in TM5, Leu809 in the TM5-6 loop, and Cys813 in TM6) as reported in the literatures [17,35-39]. The RMSF values of revaprazan-7h complex are smaller than other complexes in many active sites such as Thr134, Thr135, Asp137, Asn138, Met334, Ala335, Leu809, Trp899, Glu900, Tyr928 and Asn989 (listed in Table 2).

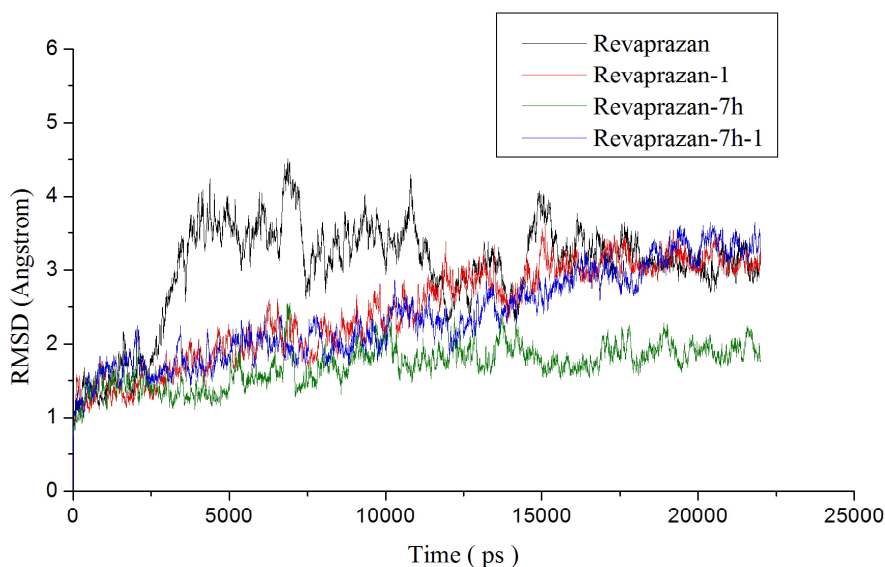


Fig.5. RMSD for the backbone atoms of the complexes: revaprazan, revaprazan-1, revaprazan-7h and revaprazan-7h-1 systems

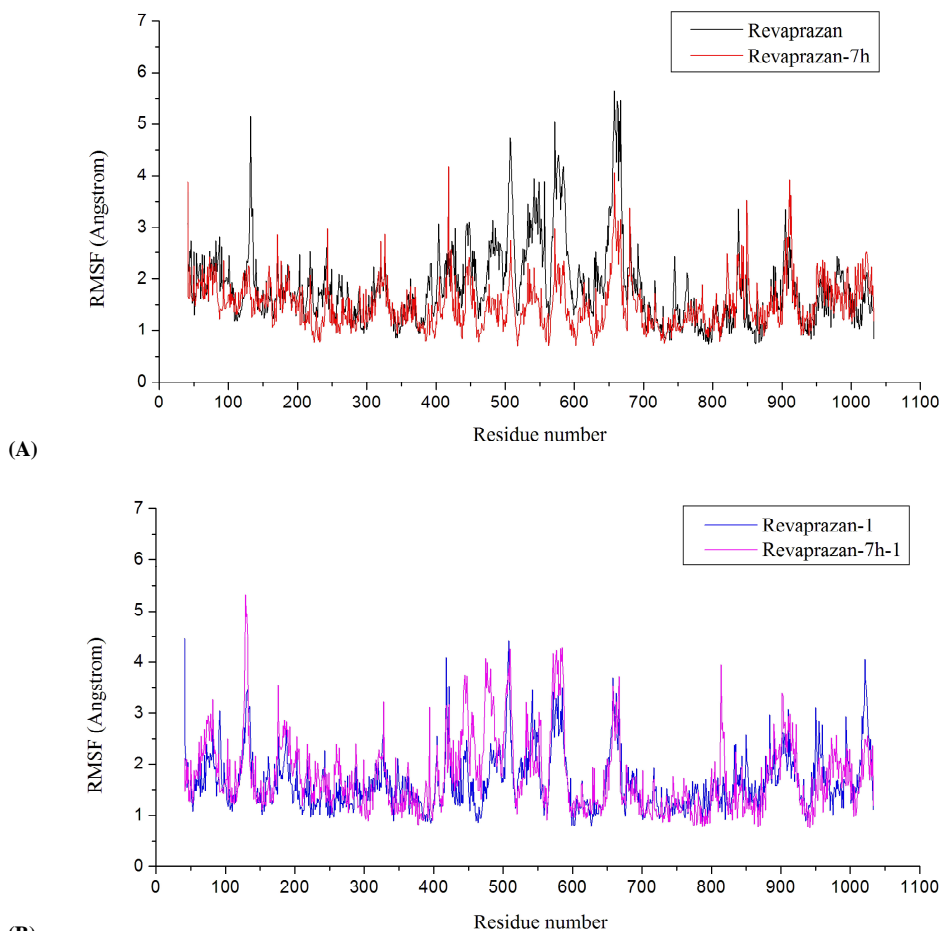


Fig.6. RMSF of each residue in the complexes: (A) revaprazan and revaprazan-7h; (B) revaprazan-1 and revaprazan-7h-1

Table 2. RMSF values (\AA) of important amino acid residues in different complex systems

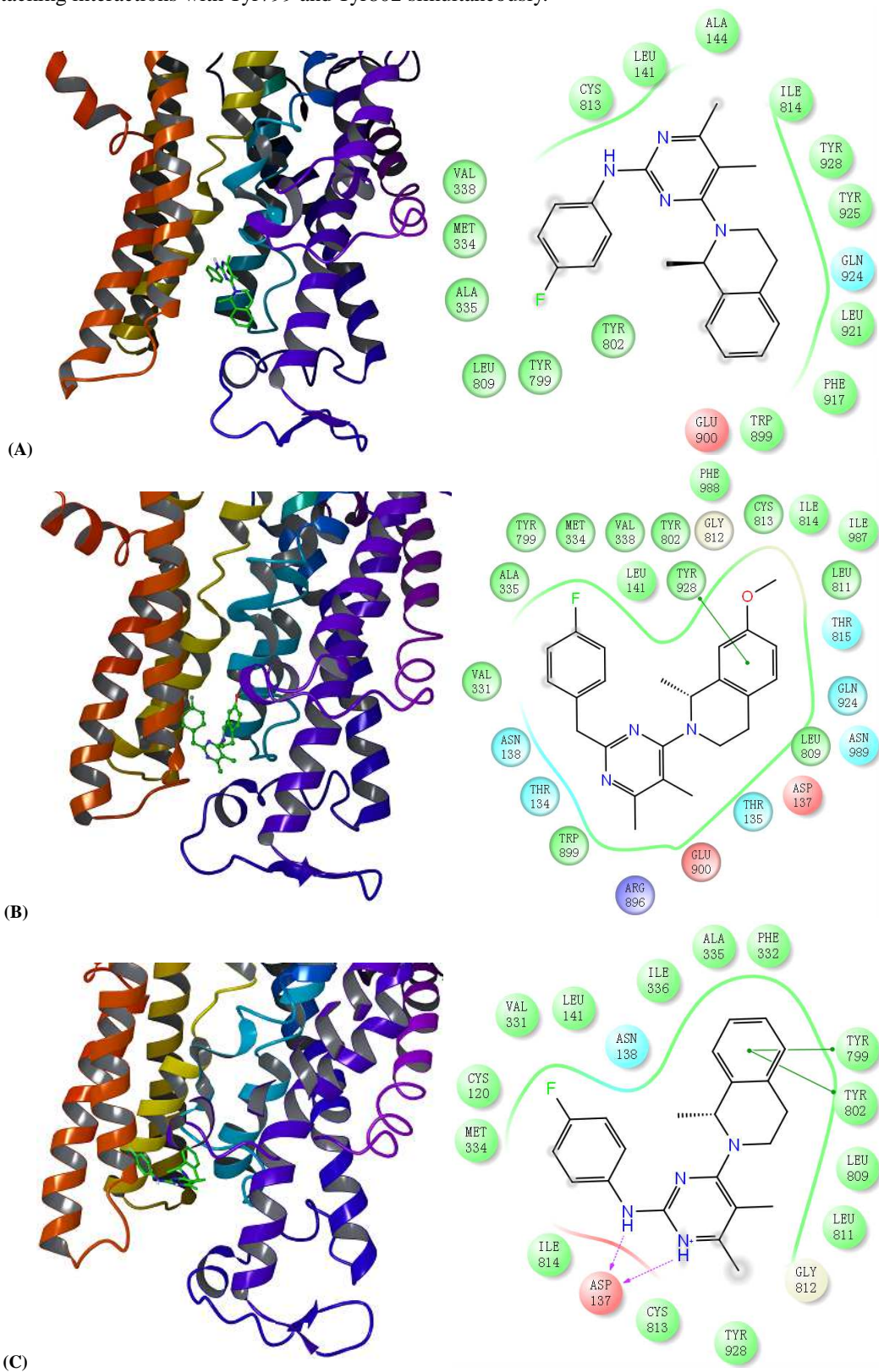
| Residue | Revaprazan | Revaprazan-7h | Revaprazan-1 | Revaprazan-7h-1 |
|---------|-------------|---------------|--------------|-----------------|
| Thr134 | 3.20 | 1.26 | 3.06 | 2.75 |
| Thr135 | 3.36 | 1.29 | 3.13 | 2.05 |
| Asp137 | 1.91 | 1.46 | 1.70 | 1.54 |
| Asn138 | 1.83 | 1.32 | 1.85 | 1.59 |
| Leu141 | 1.87 | 1.56 | 1.53 | 1.32 |
| Met334 | 1.36 | 1.35 | 1.67 | 1.67 |
| Ala335 | 1.19 | 1.08 | 1.38 | 1.19 |
| Tyr799 | 0.81 | 1.05 | 1.18 | 1.59 |
| Leu809 | 1.18 | 1.15 | 1.74 | 1.37 |
| Cys813 | 0.95 | 1.16 | 1.29 | 2.44 |
| Ile814 | 1.18 | 1.33 | 1.37 | 3.95 |
| Trp899 | 1.36 | 1.11 | 1.82 | 1.68 |
| Glu900 | 1.53 | 1.12 | 2.13 | 2.17 |
| Tyr928 | 1.08 | 0.89 | 1.32 | 1.20 |
| Phe988 | 2.16 | 1.24 | 1.14 | 1.53 |
| Asn989 | 1.79 | 1.21 | 1.49 | 1.74 |

The smallest RMSF values of residues among the complexes are bold.

Interaction modes of ligands with H^+ , K^+ -ATPase

To investigate interaction modes in the binding sites, the average structures from last 2 ns MD trajectory were compared (Fig. 7). Although both revaprazan and revaprazan-7h (neutral form) have hydrophobic interactions with the key residues Leu141, Ala335, Tyr799 and Cys813, the binding sites of revaprazan-7h are more than those of revaprazan (Fig. 7(A) and Fig. 7(B)). Compared to revaprazan, revaprazan-7h has glycine interaction with Gly812, π - π stacking interaction with Tyr928, and polar interaction with Thr134, Thr135, Asn138, Thr815 and Asn989. There are different interaction modes between protonated form and neutral form of ligand. Hydrogen atoms of imine and protonated nitrogen in revaprazan-1 formed hydrogen bonds with Asp137 (distance: $2.20 \pm 0.38 \text{ \AA}$ and $2.29 \pm 0.39 \text{ \AA}$), while revaprazan-7h-1 also has hydrogen bond with Asp137 (distance: $1.63 \pm 0.11 \text{ \AA}$) (Fig. 7(C) and Fig.

7(D)). In addition, Asp137 has negative charged interactions with all protonated ligands (+1 charged). Revaprazan-1 has π - π stacking interactions with Tyr799 and Tyr802 simultaneously.



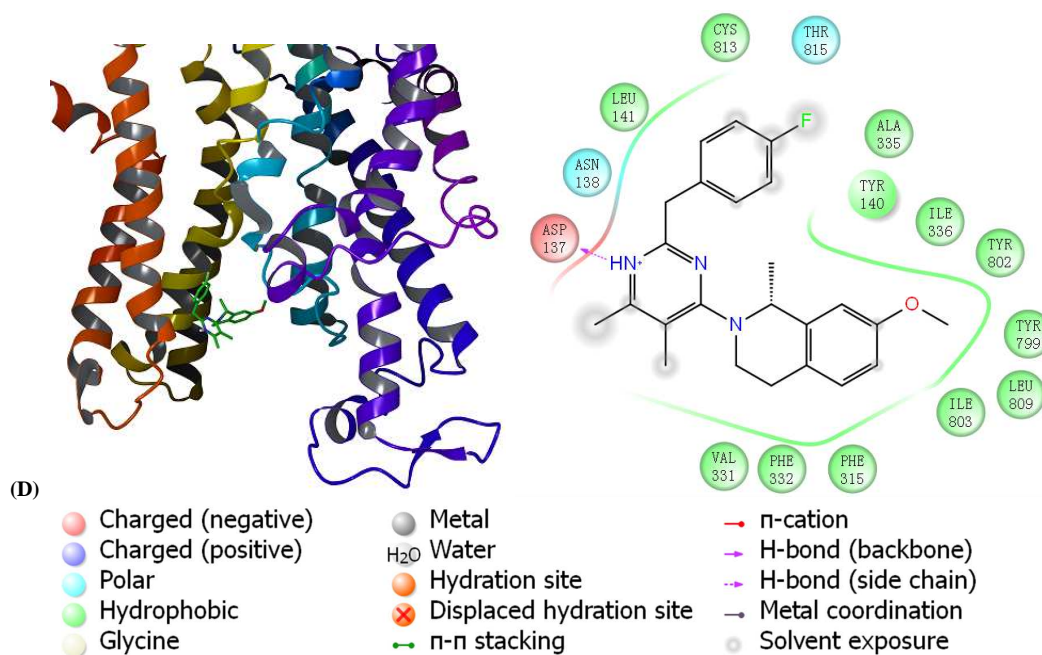


Fig.7. Interaction modes of ligands with H⁺,K⁺-ATPase: (A) revaprazan; (B) revaprazan-7h; (C) revaprazan-1; (D) revaprazan-7h-1

Binding free energy of ligands with H⁺,K⁺-ATPase

The binding free energies of all systems were calculated by MM/GBSA method. As listed in Table 3, the $\Delta G'_{\text{bind}}$ and ΔG_{bind} values show that the order of favorable binding interaction is revaprazan-7h > revaprazan-1 > revaprazan-7h-1 > revaprazan. At pH 6.1, the protonated form of revaprazan is in the majority (69.89%), while the neutral form is the principal form of revaprazan-7h (73.96%). According to the protonated form percentage of ligands, the binding free energies (ΔG_{bind}) of protonated and neutral mixtures of revaprazan and revaprazan-7h at pH 6.1 are -37.82 and -45.90 kcal/mol, respectively. It is consistent with the experimental results, which indicate that the activity of revaprazan-7h is higher than revaprazan.

From Table 3, the four individual energy components (ΔE_{Elect} , ΔE_{VDW} , ΔG_{GB} , and ΔG_{SA}) were carefully compared to estimate which energy term has most impact on the binding affinities. Both the van der Waals (ΔE_{VDW}) and the electrostatic (ΔE_{Elect}) contributions are essential for ligands binding to H⁺,K⁺-ATPase. For the neutral form, the contributions of ΔE_{VDW} are more favorable than ΔE_{Elect} term. But for the protonated form, the major favorable contributor is ΔE_{Elect} term. Among all ligands, ΔE_{VDW} and ΔG_{SA} of revaprazan-7h is the most favorable (-53.55 ± 0.8 and -4.71 ± 0.28 kcal/mol). Although ΔE_{Elect} of revaprazan-7h-1 (-78.84 ± 1.15 kcal/mol) is similar to that of revaprazan-1 (-79.41 ± 1.39 kcal/mol), ΔE_{VDW} of revaprazan-7h-1 is lower than other ligands.

Table 3. The binding free energies of ligands (kcal/mol)

| | Revaprazan | Revaprazan-7h | Revaprazan-1 | Revaprazan-7h-1 |
|------------------------------|-------------|---------------|--------------|-----------------|
| $\Delta E_{\text{internal}}$ | -0.00±0.00 | -0.01±0.00 | -0.00±0.00 | -0.00±0.00 |
| ΔE_{Elect} | -6.36±0.19 | -11.60±0.44 | -79.41±1.39 | -78.84±1.15 |
| ΔE_{VDW} | -36.08±0.34 | -53.55±0.38 | -41.38±0.38 | -34.20±0.47 |
| ΔG_{GB} | 18.80±0.26 | 19.02±0.47 | 76.31±1.27 | 75.69±0.85 |
| ΔG_{SA} | -2.12±0.21 | -4.71±0.28 | -0.75±0.32 | -1.51±0.32 |
| TΔS | -0.90±0.15 | -2.14±0.10 | -1.83±0.24 | -0.93±0.19 |
| $\Delta G'_{\text{bind}}$ | -25.76±0.40 | -50.85±0.94 | -45.23±0.50 | -38.87±0.72 |
| ΔG_{bind} | -24.86±0.37 | -48.70±0.94 | -43.40±0.54 | -37.93±0.77 |

The binding free energy between ligands and H⁺,K⁺-ATPase was decomposed into the contribution of each residue, which provides quantitative information of the key residues related to the detailed interaction mechanism. The energy comparisons of residues in binding sites are shown in Fig. 8. Besides revaprazan-7h and revaprazan have similar binding energies of residues Leu141, Met334, Ala335, Cys813, Ile814 and Glu900, the binding energies of revaprazan-7h with residues Thr134, Thr135, Val331, Tyr802, Gly812, Trp899, Gln924 and Tyr928 are more favorable than those of revaprazan (Fig. 8(A), Table 4). There is the distinct difference between protonated and neutral forms of ligands. Because of strong hydrogen bond and electrostatic interactions, the energy contributions of Asp137 to protonated form are all more favorable than those to neutral form, which reach the highest values (-19.80 ± 0.46 kcal/mol to revaprazan-1, -19.14 ± 0.35 kcal/mol to revaprazan-7h-1). The binding energies of revaprazan-7h-1 interacting with Asn138, Leu141, Ala335 and Ile336 are higher than those of revaprazan-1, while

lower than the binding energies of revaprazan-1 with Ala331, Phe332, Tyr799, Leu809, Leu811, Gly812, Cys813 and Tyr928 (Fig. 8(B), Table 4). Compared to the protonated forms (revaprazan-1 and revaprazan-7h-1), revaprazan-7h (neutral form) has strong interaction with Thr134, Thr135, Gly812, Ile814, Trp899, Glu900, Gln924, Tyr928, Phe988 and Asn989. Thus, the interaction region of revaprazan-7h (neutral form) is larger than other ligands and its binding energy is the highest. The calculation results demonstrate that enlarging the binding region of ligand would increase the activity. Using the competitive inhibitor 8-[(4-azidophenyl) methoxy]-1-trithiomethyl-2,3-dimethylimidazo-(1,2-a) pyrimidium iodide, Munson *et al.* [49] suggested the binding site included the luminal side between Gln127 and Asn138 in the TM1-2 loop of pig H⁺,K⁺-ATPase. Therefore, besides the classical binding sites such as Leu141, Ala335, Tyr799 and Cys813, the interaction with Thr134, Thr135, Asp137 and Asn138 (especially the hydrogen bond and electrostatic interactions with Asp137) should be very important for P-CABs binding to H⁺,K⁺-ATPase.

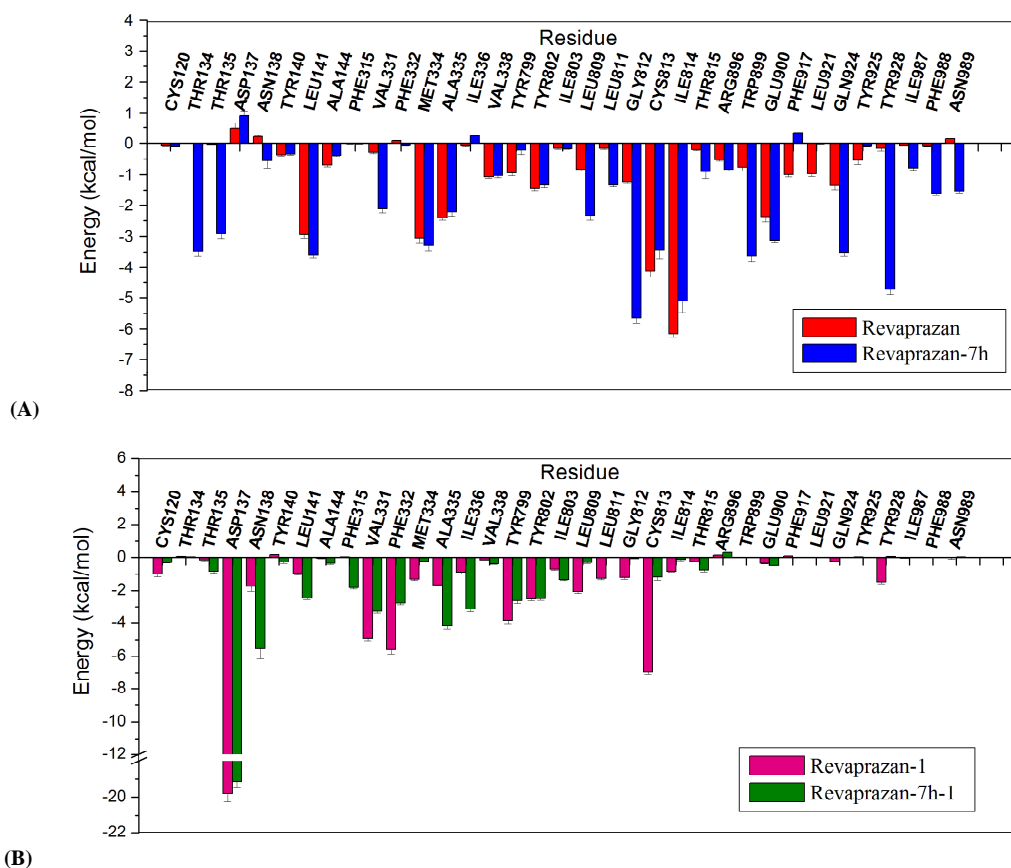


Fig.8. The comparison of energy decomposition for residues in binding sites of ligands. (A) revaprazan and revaprazan-7h; (B) revaprazan-1 and revaprazan-7h-1

Table 4 The binding energies (kcal/mol) of residues in binding sites

| Residues | Revaprazan | Revaprazan-7h | Revaprazan-1 | Revaprazan-7h-1 |
|----------|------------|---------------|--------------|-----------------|
| Thr134 | 0.00±0.00 | -3.48±0.16 | 0.06±0.01 | 0.04±0.01 |
| Thr135 | -0.03±0.01 | -2.92±0.15 | -0.15±0.04 | -0.84±0.10 |
| Asp137 | 0.48±0.18 | 0.91±0.17 | -19.80±0.46 | -19.14±0.35 |
| Asn138 | 0.22±0.04 | -0.55±0.23 | -1.73±0.29 | -5.54±0.61 |
| Leu141 | -2.95±0.11 | -3.62±0.08 | -0.96±0.07 | -2.44±0.09 |
| Val331 | -0.29±0.04 | -2.13±0.12 | -4.93±0.12 | -3.28±0.11 |
| Met334 | -3.06±0.16 | -3.30±0.16 | -1.30±0.08 | -0.22±0.02 |
| Ala335 | -2.41±0.08 | -2.23±0.14 | -1.66±0.04 | -4.16±0.20 |
| Tyr799 | -0.94±0.10 | -0.22±0.14 | -3.81±0.23 | -2.60±0.20 |
| Tyr802 | -1.44±0.08 | -1.33±0.09 | -2.49±0.12 | -2.46±0.12 |
| Leu809 | -0.82±0.04 | -2.33±0.16 | -2.04±0.11 | -0.31±0.05 |
| Leu811 | -0.17±0.02 | -1.33±0.06 | -1.25±0.09 | 0.01±0.00 |
| Gly812 | -1.22±0.06 | -5.66±0.14 | -1.21±0.11 | -0.06±0.01 |
| Cys813 | -4.13±0.20 | -3.43±0.30 | -6.96±0.13 | -1.18±0.19 |
| Ile814 | -6.15±0.11 | -5.11±0.36 | -0.82±0.04 | -0.12±0.08 |
| Trp899 | -0.76±0.11 | -3.65±0.16 | 0.00±0.03 | -0.03±0.00 |
| Glu900 | -2.38±0.16 | -3.12±0.09 | -0.37±0.02 | -0.49±0.01 |
| Gln924 | -1.34±0.15 | -3.52±0.12 | -0.24±0.03 | 0.00±0.00 |
| Tyr928 | -0.16±0.08 | -4.72±0.17 | -1.47±0.12 | 0.05±0.00 |
| Phe988 | -0.08±0.01 | -1.59±0.08 | 0.00±0.01 | 0.01±0.00 |
| Asn989 | 0.14±0.02 | -1.53±0.05 | -0.02±0.07 | 0.04±0.00 |

CONCLUSION

To compare the different interaction mechanisms between revaprazan and revaprazan-7h (neutral and protonated forms) with H⁺,K⁺-ATPase, molecular dynamics and MM/GBSA binding free energy calculations were performed. The order of favorable binding interaction is revaprazan-7h > revaprazan-1 > revaprazan-7h-1 > revaprazan. The interaction region of revaprazan-7h (neutral form) is larger than other ligands and its binding energy is the highest. Besides the classical binding sites such as Leu141, Ala335, Tyr799 and Cys813, enlarging the binding region of ligand (Thr134, Thr135, Asp137, Asn138, Trp899, Glu900, Gln924, Tyr928, Phe988 and Asn989) would increase the activity. Due to hydrogen bonds and electrostatic interactions, Asp137 in particular should be a very important binding site for protonated form of ligand. The calculation results could promote the rational design of novel P-CABs.

Acknowledgements

This work was granted by Natural Science Foundation of Hubei Province (No. 2014CFB684).

REFERENCES

- [1] H Li; L Meng; F Liu; JF Wei; YQ Wang. *Expert. Opin. Ther. Patents*, **2013**, 23, 99–111.
- [2] KS Jain; AK Shah; J Bariwal; SM Shelke; AP Kale. *Bioorg. Med. Chem.*, **2007**, 15, 1181–1205.
- [3] JM Shin; K Munson; O Vagin; G Sachs. *Pflugers. Arch. – Eur. J. Physiol.*, **2009**, 457, 609–622.
- [4] M Maeda; J Ishizaki; M Futai. *Biochem. Biophys. Res. Commun.*, **1988**, 157, 203–209.
- [5] K Hall; G Perez; D Anderson; C Gutierrez; K Munson. *Biochemistry*, **1990**, 29, 701–706.
- [6] J Lee; G Simpson; P Scholes. *Biochem. Biophys. Res. Commun.*, **1974**, 60, 825–832.
- [7] JM Wolosin. *Am. J. Physiol.*, **1985**, 248, G595–G607.
- [8] JM Shin; G Sachs. *Dig. Dis. Sci.*, **2006**, 51, 823–833.
- [9] K Andersson; E Carlsson. *Pharmacol. Ther.*, **2005**, 108, 294–307.
- [10] G Sachs; JM Shin; O Vagin; N Lambrecht; I Yakubov. *J. Clin. Gastroenterol.*, **2007**, 41, S226–242.
- [11] G Sachs; JM Shin; CW. *Aliment. Pharmacol. Ther.*, **2006**, 23, S2–8.
- [12] JW Lee; JS Chae; CS Kim; JK Kim; DS Lim. *US005750531A*, **1998**.
- [13] W Li; Y Yang; Y Tian; X Xu; Y Chen. *Int. J. Pharm.* **2011**, 408, 157–162.
- [14] YA Yoon; CS Park; MH Cha; H Choi; JY Sim. *Bioorg. Med. Chem. Lett.* **2010**, 20, 5735–5738.
- [15] ACD/I-Lab, version 12.01, Advanced Chemistry Development, Inc., Toronto, ON, Canada, **2013**. www.acdlabs.com
- [16] K Abe; K Tani; T Nishizawa; Y Fujiyoshi. *Embo. J.*, **2009**, 28, 1637–1643.
- [17] K Abe; K Tani; Y Fujiyoshi. *Nat. Commun.*, **2011**, 2, 155–160.
- [18] M Maeda; K Oshiman; S Tamura; M Futai. *J. Biol. Chem.*, **1990**, 265, 9027–9032.
- [19] HM Berman; J Westbrook; Z Feng; G Gilliland; TN Bhat. *Nucleic Acids Res.*, **2000**, 28, 235–242.
- [20] T Shinoda; H Ogawa; F Cornelius; C Toyoshima. *Nature*, **2009**, 459, 446–450.
- [21] SF Altschul; TL Madden; AA Schaffer; J Zhang; Z Zhang. *Nucleic Acids Res.*, **1997**, 25, 3389–3402.
- [22] R Chenna; H Sugawara; T Koike; R Lopez; TJ Gibson. *Nucleic Acids Res.*, **2003**, 31, 3497–3500.

- [23] A Sali; TL Blundell. *J. Mol. Biol.*, **1993**, 234, 779–815.
- [24] Schrödinger, LLC, New York, **2010**. www.schrodinger.com
- [25] WL Jorgensen; DS Maxwell; J Tirado-Rives. *J. Am. Chem. Soc.*, **1996**, 118, 11225–11236.
- [26] RA Laskowski; MW MacArthur; DS Moss; JM Thomson. *J. Appl. Crystallogr.*, **1993**, 26, 283–291.
- [27] LigPrep, version 2.4, Schrödinger, LLC, New York, NY, **2010**.
- [28] JC Shelley; A Cholleti; L Frye; JR Greenwood; MR Timlin. *J. Comp-Aided Mol. Design*, **2007**, 21, 681–691.
- [29] W Sherman; T Day; MP Jacobson; RA Friesner; R Farid. *J. Med. Chem.*, **2006**, 49, 534–553.
- [30] H Zhong; LM Tran; JL Stang. *J. Mol. Graph. Model.*, **2009**, 28, 336–346.
- [31] H Wanga; R Aslanian; VS Madison. *J. Mol. Graph. Model.*, **2008**, 27, 512–521.
- [32] HJ Luo; JZ Wang; WQ Deng; K Zou. *Med. Chem. Res.*, **2013**, 22, 4970–4979.
- [33] Glide, version 5.6, Schrödinger, LLC, New York, NY, **2010**.
- [34] RA Friesner; RB Murphy; MP Repasky; LL Frye; JR Greenwood. *J. Med. Chem.*, **2006**, 49, 6177–6196.
- [35] O Vagin; S Denevich; K Munson; G Sachs. *Biochemistry*, **2002**, 41, 12755–12762.
- [36] K Munson; C Gutierrez; VN Balaji; K Ramnarayan; G Sachs. *J. Biol. Chem.*, **1991**, 266, 18976–18988.
- [37] S Asano; S Matsuda; Y Tega; K Shimizu; S Sakamoto. *J. Biol. Chem.*, **1997**, 272, 17668–17674.
- [38] O Vagin; K Munson; N Lambrecht; SJD Karlish; G Sachs. **2000**, 40, 7480–7490.
- [39] K Munson; RJ Law; G Sachs. *Biochemistry*, **2007**, 46, 5398–5417.
- [40] MP Jacobson; DL Pincus; CS Rapp; TJF Day; B Honig. *Proteins*, **2004**, 55, 351–367.
- [41] Desmond Molecular Dynamics System, Version 3.1, D.E. Shaw Research, New York, NY, **2012**.
- [42] D Shivakumar; J Williams; Y Wu; W Damm; J Shelley. *J. Chem. Theory Comput.*, **2010**, 6, 1509–1519.
- [43] W Humphrey; A Dalke; K Schulten. *J. Mol. Graph.*, **1996**, 14, 33–38.
- [44] The PyMOL molecular graphics system, Version 1.5. Schrödinger, LLC, **2012**.
- [45] Maestro, version 9.3, Schrödinger, LLC, New York, NY, **2012**.
- [46] PA Kollman; I Massova; C Reyes; B Kuhn; S Huo. *Acc. Chem. Res.*, **2011**, 33, 889–897.
- [47] I Massova; PA Kollman. *Perspect. Drug Discov. Des.*, **2000**, 18, 113–135.
- [48] MacroModel, version 9.8, Schrödinger, LLC, New York, NY, **2010**.
- [49] KB Munson; C Gutierrez; VN Balaji; K Ramnarayan; G Sachs. *J. Biol. Chem.*, **1991**, 266, 18976–18988.